THE ASTRONOMICAL JOURNAL VOLUME 105, NUMBER 5 MAY 1993

PROPER MOTIONS, MEMBERSHIP, AND PHOTOMETRY OF OPEN CLUSTERS NEAR ETA CARINAE

KYLE M. CUDWORTH AND STEVEN C. MARTIN

Yerkes Observatory, The University of Chicago, P.O. Box 258, Williams Bay, Wisconsin 53191
Electronic mail: kmc@yerkes.uchicago.edu, smartin@oddjob.uchicago.edu

KATHLEEN DEGIOIA-EASTWOOD

Department of Physics and Astronomy, Northern Arizona University, P.O. Box 6010, Flagstaff, Arizona 86011
Electronic mail: eastwood@nauvax.bitnet

Received 1992 November 24; revised 1993 January 19

ABSTRACT

Proper motions and photographic photometry have been derived for nearly 600 stars with $7.5 < V < 15.5$ in the region of the very young open clusters Tr 14, Tr 16, and Cr 232 based on 26 plates dating from 1893 to 1990. Cluster membership probabilities have been derived from the proper motions and color–magnitude diagrams of probable members of each cluster are presented. In contrast to a few of the previous studies we find all three clusters to lie at the same distance.

1. INTRODUCTION

The region in and around the Carina Nebula (NGC 3372) contains a wealth of apparently very young open clusters. Investigations in this region of the sky have centered on the relations between the clusters, gas, and dust (see, for example, Feinstein *et al.* 1973; Walborn 1973; Tapia *et al.* 1988) and whether or not the extinction law within the clusters is anomalous (Smith 1987; Garcia *et al.* 1988; Herbst 1976; Turner & Moffat 1980). The importance of these investigations lies in various aspects of star and cluster formation theory and the effects of intense radiation fields from young OB type stars on grains in the nearby dust clouds.

Observations in visible wavelengths of various stars in the Carina complex have been steadily improved and enlarged through spectral classification and photometry by various researchers (Feinstein *et al.* 1973; Feinstein 1982; Turner & Moffat 1980; Forte & Orsatti 1981; Levato & Malaroda 1982; Walborn 1982, and references therein; Morrell *et al.* 1988; Massey & Johnson 1993). Despite all of this data, there has been some controversy over whether or not Tr 14 and Tr 16 lie at the same distance. Walborn (1973) found that Tr 16 lies considerably closer than Tr 14 (2.6 kpc for Tr 16, as opposed to 3.5 kpc for Tr 14). In contrast, Turner & Moffat (1980), Tapia *et al.* (1988), and Massey & Johnson (1993) concluded Tr 14 and Tr 16 are actually at the same distance (though that distance ranges between $\sim$2.4 and $\sim$3.2 kpc among these papers). Turner *et al.* (1980) studied the neighboring cluster NGC 3293 and its relationship to other young clusters in the vicinity, concluding that all lie at essentially the same distance. It should be noted that the reason, in part, for the conflicting distance estimates is the nature of the extinction in and around these clusters. For example, Morrell *et al.* (1988) pointed out that the HR diagram for Tr 14 lies approximately 1 mag lower than that of Tr 16. This could be interpreted as either due to different distances of the clusters, or different extinctions within each cluster. Further, it is naturally assumed that stars within each cluster are physically associated, having presumably formed out of the same molecular cloud. However, any study of the clusters will contain stars which are intrinsic to the cluster, plus some nonmembers simply along the same line of sight. Questions of cluster membership have not been adequately dealt with. To date, the probable members of each cluster have been deduced based on an analysis of color–color diagrams for the clusters (see, for example, Feinstein *et al.* 1973).

In order to better address questions concerning the relationship among the clusters, it is necessary to systematically determine the cluster membership of stars in these regions independent of possible photometric biases. In this paper, we present proper motions and membership probabilities as well as photographic B and V photometry for nearly 600 stars in the regions of Tr 14, Tr 16, and Cr 232. In Sec. 2, the observations and measurements are reviewed, while in Sec. 3 the astrometric and photometric reductions are described. Section 4 discusses the color–magnitude diagrams (CMD's), the kinematic relationship between the clusters, the distribution of members within the clusters, and some comments on implications for previous studies of these clusters. Conclusions are summarized in Sec. 5.

2. OBSERVATIONS AND MEASUREMENTS

The plates used in this study span approximately a century at three different epochs. These plates are listed in Table 1 along with their scales, epochs, and passbands. Note the following telescope designations: X, Harvard 13 in. refractor in Arequipa, Peru; SB, Harvard 60 in. reflector in South Africa; CF, Las Campanas 1 m reflector; CD, Las Campanas 2.5 m reflector. The X and SB series plates were unfiltered blue plates and for the X series the pass-

 0004-6256/93/051822-09$00.90

TABLE 1. η Car plate material.

Plate no.	Scale	Epoch	Color
X-4604	42.35	1893.32	b
X-4634	42.35	1893.33	b
X-4635	42.35	1893.33	b
X-4669	42.35	1893.36	b
X-5554	42.35	1894.39	b
X-5720	42.35	1894.56	b
X-6969	42.35	1895.59	b
X-8292	42.35	1897.07	b
SB-1037	26.18	1937.33	b
SB-1038	26.18	1937.33	b
SB-1361	26.18	1938.24	b
SB-1373	25.90	1938.32	b
SB-2209	26.18	1940.18	b
SB-2233	26.18	1940.27	b
CF-4845	29.03	1986.30	V
CF-4946	29.03	1986.30	V
CF-4956	29.03	1986.30	V
CF-4957	29.03	1986.30	V
CF-4958	29.03	1986.30	V
CF-4959	29.03	1986.30	V
CF-4962	29.03	1986.44	B
CF-4963	29.03	1986.44	B
CF-4974	29.03	1986.44	B
CF-4965	29.03	1986.44	B
CF-4966	29.03	1986.45	B
CD-2861	10.92	1990.18	B
CD-2878	10.92	1990.19	V
CD-2879	10.92	1990.19	V

band was very close to *B* in Johnson's *UBV* standard system. Since the SB plates were taken with a reflector their passband probably included a good deal more ultraviolet than does standard *B*. All of the 1986 Las Campanas *V* exposures were taken on IIa-D plates with a GG495 filter, while the *B* passband was matched by using IIa-O plates and a GG385 filter. The newest Las Campanas plates are either 103a-O (plus GG385 filter) to match *B* or 103a-D (with GG495 filter) to match *V*. SB-1373 was taken with a coma corrector yielding a slightly different scale from the other SB plates, as well as probably a different passband due to UV absorption by the glass.

Stars were selected from a Las Campanas (CF) blue plate and cover an area of approximately 375 square arcmin including the clusters Tr 14, Tr 16, and Cr 232. Figure 1 (Plate 88) is a reproduction from a Las Campanas blue plate (CF-4963) showing this region. Stars at the center of Tr 14 were excluded due to excessive crowding of the images. Further, η Carinae itself was not included due to the peculiar nonstellar nature of this image. In all, 577 stars were included, in a magnitude range of $7 \lesssim V \lesssim 16$.

All of the plates were scanned on the PDS microdensitometer at MADRAF (Midwest Astronomical Data Reduction and Analysis Facility) in Madison, Wisconsin. The procedure (which is now standard at MADRAF for astrometric/photometric studies) involves scanning a small region centered on each star. After initial reductions of the data at MADRAF, actual photometric and astrometric reductions were done at Yerkes Observatory with the software described by Cudworth (1985, 1986).

3. REDUCTIONS

3.1 Photometry

Photometry of all stars in our sample was needed in order to properly reduce the astrometry as well as for astrophysical interpretation of our results. Preliminary photometric reductions were run to obtain approximate colors needed for the astrometry, and later improved upon after the astrometric reductions (in which bad images were identified and removed from the reduction). To obtain the best possible photometry, only the newest plates (Las Campanas 1986 CF series, and 1990 CD series) were used. Previous experience has shown that older plates very similar to those used here are usually less reliable for photometry due to nonuniformity of the emulsions or the photographic processing. The final step in the photometric reduction was the transformation to the photoelectric system. The photoelectric standard stars were chosen from Feinstein *et al.* (1973) and Feinstein (1982) and included only those stars which were believed to be "normal" (possible variable stars and peculiar stars excluded). Since these photoelectric studies did not reach as faint as our data, an extrapolation of about a magnitude was required in this calibration. Accidental errors in the final photometry for stars with clean, uncrowded, images (without significant nebular contamination) range from $\epsilon(V, B-V) \approx \pm(0.01, 0.02)$ for the brighter stars ($V \lesssim 13$) to $\epsilon(V, B-V) \approx \pm(0.03, 0.06)$ for the faintest stars. While these accidental errors may be comparable those of the Massey & Johnson (1993) CCD photometry, our precision is poorer for crowded or contaminated images and our photometry is more susceptible to systematic errors at the faint end.

3.2 Astrometry

Proper motion reductions followed the technique described by Cudworth (1985,1986). In this iterative central overlap reduction we included linear and quadratic terms in the coordinates and in magnitude, as well as coma terms (magnitude times coordinate), linear color, and color magnification (color times coordinate). The Las Campanas CD and CF series plates were taken through correctors which introduce mild distortion that was removed prior to the plate constant reductions using the calibrations derived by Cudworth & Rees (1991). Distortion terms were included in the plate constants to remove any slight remaining distortion not removed by this precorrection. Significant distortion was, of course, found for SB-1373 due to the use of a coma corrector for this plate. During the initial reductions, stars were identified which had high residuals. These stars were then examined on the original plates to check for poor images (due to emulsion imperfections, scratches, faintness, or two or more images blended together). Those images found unsatisfactory were subse-

TABLE 2. Probability parameters for η Car region.

Parameter	Cluster	Field
N	353	210
μ_{x0}	0".00 cent^{-1}	0".00 cent^{-1}
μ_{y0}	0".00	0".00
σ_x	0".0.75	0".42
σ_y	0".0.75	0".24

quently deleted from the data set. Once preliminary proper motions were determined, very high proper motion stars were identified and removed from the initial plate constant derivation. The importance of removing such stars has been emphasized by Cudworth (1976), who has shown that high proper motion stars can adversely skew the plate constants.

The probability of membership for each star was derived using the procedure originally developed by Vasilevskis *et al.* (1958) and later modified by Dr. E. Green (see description by Cudworth 1985). Various parameters to the Gaussian fits are displayed in Table 2, where N denotes the number of stars in the distribution, μ_{x0} and μ_{y0} refer to the centers of the distribution, while σ_x and σ_y are the standard deviations (all in units of arcseconds per century).

After all of the photometric and astrometric reductions were completed, a search for possible systematic errors in the proper motions was carried out. Proper motions of highly probable members were plotted against quantities such as magnitude and color. A few mildly significant trends, particularly a magnitude term for the brightest stars, were found to be significant, first from these plots and then from least-squares fits to the proper motions. The proper motions of all the stars were then corrected to eliminate these systematic trends and membership probabilities were rederived. Very few stars showed any significant change in membership probability after these corrections.

A compilation of the photometry, astrometry, and membership probabilities is presented in Table 3, the primary results of this study. The first column gives the star identification number: prefix FA, Feinstein *et al.* (1973); FB, Feinstein (1982); HD, *Henry Draper Catalogue;* Y, this study. The next two columns lists the x and y coordinates in arcseconds relative to the star Y1, which we find to lie at $(\alpha,\delta) = 10^h42^m\ 32^s.87,\ -59°20'29''.0$ (1950) from reductions of this star against several stars from the SAO catalog measured on Las Campanas 1 m plates. The (x,y) coordinate system is closely aligned with α,δ (equinox 1950) and the positions are given for epoch 1975). The following four columns show relative proper motions and their errors in units of milliarcseconds per century (mas cent^{-1}, or 10^{-5} arcsec yr^{-1}). Columns 7 and 8 list the photometry (V and $B-V$), and the final column is the calculated membership probability (P) in percent. Inspection of this final column shows a quite good segregation between probable members and nonmembers.

4. DISCUSSION

4.1 The Color–Magnitude Diagram

Our photometric data for all of the stars measured was used to construct the CMD shown in Fig. 2(a). In Fig. 2(b), the stars are segregated according to their membership probabilities (filled circles represent stars with $P \geqslant 80\%$, whereas open circles refer to stars with $20\% \leqslant P < 80\%$). The usefulness of the membership probabilities is fairly obvious. These CMD's are consistent with previously published diagrams, such as Feinstein *et al.* (1973), which show a clearly defined main sequence, but little (or no) indication of a turnoff at the bright end. Much of the scatter along the main sequence should be attributed to differential reddening, not to photometric uncertainties. As may be seen in Fig. 2(b), some stars with high membership probabilities appear to lie far to the right of the main sequence. A few of these stars are discussed further below. It should be noted, however, that some of these stars may be nonmembers despite their high membership probability. On statistical grounds it is expected that $\sim$20 of the 291 stars with $P \geqslant 80\%$ and $\sim$50 of the 112 stars with $20\% \leqslant P < 80\%$ may be nonmembers.

Shown in Figs. 2(c) through 2(e) are CMD's of stars in each of the three regions Tr 14, Tr 16, and Cr 232, respectively. The stars considered associated with each of these regions were selected by position, with our boundaries of the three regions agreeing roughly with those found in the literature (for example, Feinstein *et al.* 1973).

It has recently been argued by Morrell *et al.* (1988) that the HR diagram for Tr 14 lies approximately 1 mag below that of Tr 16. Of the 28 stars assigned to Tr 16 by them, 18 were identified with stars in our survey, of which 17 had membership probabilities $P > 90\%$. Of the 7 stars they observed in Tr 14, only 4 common to our study and 3 of these have $P > 90\%$. Thus, we conclude that the possibility of contamination by foreground stars is probably not significant and the author's conclusion of a shift in the diagrams for Tr 14 and Tr 16 is probably not due to field star contamination of the CMD's. However, their sample of stars was limited to the brightest members in the cluster ($V \lesssim 11$). Our survey contains considerably more stars and extends down to $V \sim 15.5$, where the main sequence is much less vertical. If all the stars with high membership probabilities in our study are used to search for a shift in the CMD's of the clusters, no clear shift is evident (and certainly not at the level of about 1 mag). We thus argue that the clusters are most probably at the same distance with reasonably similar reddening and extinction. The crucial difference between our study and Morrell *et al.* is that our CMD's are not limited to the very bright stars where the main sequence is nearly vertical but rather reach faint enough that vertical shifts are much easier to investigate. Massey & Johnson (1993) also find the clusters to lie at the same distance from their recent CCD photometry and spectroscopy.

The above differential comparisons of our CMD's are rather easily done and are not sensitive to possible system-

TABLE 3. Positions, proper motions, photometry, and membership probabilities.

Names	X	Y	μ_x	ϵ_x	μ_y	ϵ_y	V	B-V	P	Names	X	Y	μ_x	ϵ_x	μ_y	ϵ_y	V	B-V	P
	arcsec		milliarcsec cent^{-1}						%		arcsec		milliarcsec cent^{-1}						%
HD92350	118.4	141.4	-215	31	96	34	7.50	0.16	24	FA58	-9.2	-240.6	34	19	-40	20	12.46	0.27	96
HD93162	-142.4	-416.4	-79	30	-11	30	8.01	0.44	93	Y602	-364.1	259.7	51	20	-49	21	12.46	0.28	95
HD303308	277.1	-229.8	-31	21	-108	28	8.21	0.11	90	FA28	-348.6	130.4	8	20	11	20	12.46	0.41	96
FA100	95.4	-640.8	-20	28	-47	28	8.52	0.20	95	FA41	206.8	-247.6	90	31	-108	30	12.48	0.37	81
FA104	136.7	-457.5	-28	21	-15	18	8.75	0.18	96	FA68	275.4	-307.7	-36	24	4	44	12.50	0.26	95
HD303311	60.8	200.5	7	19	9	13	8.90	0.11	96	Y 3	-534.0	46.8	-269	14	-985	16	12.51	0.50	0
FA110	329.9	-483.2	-29	21	37	17	9.17	0.31	96	FA59	-82.9	-374.4	-24	14	37	17	12.52	0.22	96
HD93268	175.2	173.2	-453	12	174	18	9.22	0.04	0	Y476	-37.5	50.3	14	14	-26	15	12.52	0.23	96
FA112	357.4	-440.9	-39	14	41	15	9.22	0.29	96	Y610	-236.7	365.1	-574	32	263	23	12.52	0.30	0
FA34	328.6	-510.2	-12	33	15	39	9.43	0.21	96	Y317	-191.6	-719.8	19	19	-63	17	12.53	0.42	95
FA36	-106.3	-449.0	403	17	-36	19	9.47	1.65	0	Y189	375.6	-362.2	-73	22	37	17	12.57	0.31	94
FA20	-325.0	199.3	-3	21	-9	18	9.55	0.28	96	Y543	-246.0	246.5	-15	18	15	29	12.64	0.25	96
HD93343	325.0	-524.3	-2	24	-18	27	9.58	0.21	96	Y537	-203.4	226.4	-7	32	72	22	12.65	0.31	94
FA9	276.6	-411.6	22	11	55	16	9.70	0.25	95	Y307	-42.9	-591.9	-204	19	104	17	12.65	0.36	27
FA10	7.6	-70.9	-30	17	39	15	9.71	0.23	96	Y544	-261.8	255.7	-119	16	97	27	12.66	0.74	78
Y579	-446.7	409.5	107	21	-116	16	9.85	0.26	77	FA52	295.4	-151.2	66	24	22	18	12.68	0.35	95
FA35	3.4	237.4	-2672	25	-318	16	9.91	1.11	0	FA123	-87.8	211.4	-41	20	0	23	12.70	0.23	96
FA94	-21.1	-287.4	-27	22	55	13	9.92	0.06	95	Y 53	45.4	153.1	-427	29	249	35	12.70	1.07	0
Y494	-476.5	-72.2	-779	28	112	22	9.97	0.03	0	Y272	254.7	-733.4	-32	26	61	26	12.70	1.12	94
Y500	-425.4	62.2	124	25	60	17	10.01	0.50	83	Y461	-198.4	-83.2	-16	23	-128	21	12.71	0.28	87
FA115	388.0	-395.0	-18	15	17	13	10.03	0.13	96	Y 71	147.2	205.9	8	18	19	14	12.71	0.21	96
FA20	71.9	-718.7	30	14	-41	21	10.12	-0.01	96	Y154	469.5	-297.1	-10	21	5	21	12.71	0.37	96
FA3	283.3	-340.4	4	10	31	15	10.12	0.20	96	Y261	332.9	-536.3	-3535	27	223	35	12.72	0.61	0
Y611	-206.2	398.1	-34	17	-32	16	10.12	0.17	96	Y284	4.2	-700.8	6	14	66	16	12.72	0.09	95
Y297	-10.2	-546.5	-724	15	872	16	10.16	0.96	0	Y216	173.5	-485.4	-11	17	-41	24	12.73	0.40	96
FA31	203.8	192.8	41	14	22	9	10.32	0.18	96	Y 87	289.6	151.3	16	29	300	26	12.75	1.17	3
FA127	-216.1	28.9	6	19	35	14	10.67	0.37	96	FA63	67.8	-410.0	-37	19	24	21	12.77	0.26	96
Y547	-309.7	169.9	-106	24	92	35	10.74	0.44	81	Y509	-311.6	-14.4	483	27	-930	26	12.79	0.75	0
FA16	83.5	-333.1	33	25	43	15	10.77	0.25	95	Y 1	0.0	0.0	-507	14	-950	21	12.82	0.75	0
Y398	-121.4	-415.4	84	38	65	21	10.80	0.92	89	FA39	216.4	-223.9	71	33	18	26	12.83	0.45	94
FA8	256.2	-236.4	-23	27	-78	20	10.88	0.15	94	Y155	495.5	-267.3	1822	21	-642	18	12.84	0.39	0
Y 28	-37.3	339.6	-26	13	-31	13	10.88	0.21	96	Y346	-34.9	-483.3	-32	17	-8	20	12.85	0.24	96
FA21	57.0	-674.3	80	18	-23	21	10.89	0.45	94	Y436	-150.0	-144.4	-88	17	15	30	12.86	0.24	93
FA22	294.8	-591.0	55	19	-31	22	10.97	0.48	95	Y499	-473.7	28.6	24	32	-306	16	12.88	1.30	2
FA13	27.2	-250.3	-31	35	-20	32	10.99	0.16	95	FA51	292.1	-164.7	25	25	-44	25	12.89	0.30	95
FA126	-224.3	50.3	4	26	17	18	11.00	0.41	96	Y331	-169.5	-635.9	60	19	55	21	12.89	1.22	94
FA17	9.2	-325.0	13	16	22	13	11.00	0.20	96	Y116	328.4	-170.1	13	17	-46	16	12.90	0.37	96
FA27	357.2	-220.4	-15	10	-30	21	11.07	0.15	96	FA47	168.9	-417.6	18	16	-16	21	12.90	0.34	96
FA32	106.1	213.5	273	13	-440	14	11.08	0.13	0	FA50	113.7	-377.4	107	23	-62	21	12.91	0.32	87
Y322	-127.3	-702.7	389	17	-7	19	11.18	1.41	0	Y 70	126.7	192.0	2	22	-17	18	12.91	0.24	96
FA30	213.4	-22.8	495	17	-440	13	11.18	1.01	0	Y163	391.7	-328.2	22	22	20	13	12.92	0.43	96
Y 2	211.0	321.5	139	9	200	10	11.18	0.07	19	Y106	411.2	-53.4	-54	16	-27	27	12.92	1.37	95
FA124	-179.1	63.2	31	15	-31	13	11.19	0.19	96	Y 68	80.5	144.5	-1870	24	261	22	12.92	0.48	0
FA76	328.0	-392.6	-17	17	25	18	11.20	0.42	96	Y285	47.9	-713.0	-38	22	110	13	12.93	0.14	90
FA11	-51.6	-190.2	70	14	-85	20	11.23	0.16	91	Y 33	62.0	404.3	2	21	-19	19	12.93	0.24	96
Y530	-242.2	155.9	21	21	-76	12	11.24	0.18	94	FA57	-41.8	-291.1	-52	34	-41	23	12.93	0.37	94
Y551	-260.3	179.7	33	13	-51	36	11.24	0.21	95	Y266	330.5	-590.0	-19	17	-21	18	12.93	0.42	96
Y558	-346.0	147.7	123	46	-32	33	11.27	0.30	81	Y443	-209.9	-250.8	66	21	-34	17	12.93	0.18	94
Y533	-224.7	183.8	52	25	-3	26	11.28	0.24	95	Y489	-260.9	-9.8	44	25	-44	21	12.95	0.35	95
Y613	-161.9	375.6	-75	17	41	16	11.32	0.23	94	Y 92	140.3	2.9	-42	24	0	28	12.98	0.32	96
FA122	-30.2	186.2	-3	16	-5	16	11.34	0.20	96	Y 21	-20.5	144.7	-25	23	24	25	12.98	0.33	96
Y550	-272.2	165.9	-5	16	10	19	11.43	0.34	96	FA42	220.2	-207.4	-133	30	-63	22	12.98	0.41	79
Y581	-384.3	411.4	-35	21	-25	21	11.43	1.26	96	Y142	562.7	-217.7	-66	22	61	18	12.99	0.33	93
Y 38	278.6	293.6	-147	17	69	33	11.43	0.30	73	Y453	-369.0	-143.1	226	23	-192	18	12.99	0.51	3
FA15	88.3	-234.4	17	21	-12	17	11.44	0.38	96	Y523	-131.4	144.0	-30	18	39	16	13.00	0.36	96
FA29	184.9	-92.1	-76	17	13	19	11.48	0.43	94	FA54	352.4	-119.3	1065	22	-557	29	13.01	0.52	0
Y273	223.6	-785.2	49	14	-22	20	11.51	0.03	96	FA11	-252.9	226.6	-149	40	156	38	13.02	0.59	38
FA12	0.6	-142.3	-3	24	-22	23	11.56	0.29	96	Y320	-159.5	-704.1	297	17	-293	17	13.03	0.54	0
FA24	276.9	-482.7	-39	12	-15	13	11.58	0.16	96	FA69	291.9	-317.9	20	25	-49	21	13.03	0.41	95
Y452	-430.4	-167.1	105	21	108	24	11.61	0.22	79	Y 49	23.1	166.6	76	26	-79	31	13.05	0.40	89
Y107	399.8	-82.0	17	17	-39	20	11.63	0.25	96	Y166	338.4	-325.7	5	19	33	16	13.07	0.38	96
FA25	234.3	-438.4	-9	17	8	16	11.64	0.25	96	Y 9	-78.3	358.5	-170	21	39	18	13.07	0.17	66
FA46	224.0	-367.0	23	15	-72	14	11.67	0.33	95	Y292	127.7	-590.0	27	21	25	18	13.07	0.26	96
FA74	306.0	-401.0	-17	10	-14	14	11.68	0.27	96	Y364	82.8	-444.5	8	23	-13	22	13.07	0.31	96
Y280	56.5	-812.2	-293	16	159	16	11.72	0.10	0	Y321	-133.6	-716.3	332	15	-48	20	13.08	0.15	0
Y203	345.7	-427.1	-11	20	12	17	11.72	0.35	96	Y151	478.4	-379.6	-19	19	-8	25	13.08	0.51	96
Y582	-331.1	400.3	83	21	85	19	11.76	1.02	89	Y445	-227.6	-221.9	-328	26	-99	27	13.08	1.31	0
Y 56	53.2	60.8	-19	21	-24	18	11.79	1.32	96	Y238	520.0	-473.3	55	19	20	29	13.09	0.78	95
Y202	358.7	-417.9	-8	15	70	21	11.82	0.36	95	FA25	-247.6	119.9	-21	18	61	29	13.12	0.32	95
FA6	216.4	-286.9	8	17	-23	12	11.84	0.20	96	Y201	332.5	-411.7	-433	27	-72	23	13.14	0.64	0
Y413	-154.4	-302.6	-597	19	195	16	11.84	0.61	0	Y351	116.3	-477.8	-43	18	-70	18	13.15	0.28	94
Y192	403.1	-380.5	42	19	27	18	11.89	0.25	96	Y227	199.7	-541.8	-542	26	120	20	13.16	0.56	0
FA14	59.5	-225.6	-16	12	-28	24	11.89	0.36	96	FA49	87.4	-426.0	163	25	16	29	13.18	1.77	71
FA73	280.4	-379.7	-21	12	3	17	11.91	0.39	96	Y519	-194.4	100.3	-126	27	-27	33	13.18	0.29	85
FA48	119.5	-430.1	48	17	-7	15	11.92	0.19	96	Y344	-54.3	-484.6	-2039	31	-740	26	13.20	0.77	0
FA26	231.7	-418.8	5	12	-36	14	11.98	0.18	96	Y528	-157.9	146.0	-7	37	84	30	13.20	0.35	93
Y349	16.3	-472.6	-60	28	49	25	12.05	0.18	94	FA45	101.4	-112.2	-1711	24	2341	23	13.21	0.78	0
Y516	-239.3	140.8	27	18	-67	21	12.07	0.30	95	Y245	543.7	-607.3	-1167	37	-1042	32	13.21	0.63	0
Y542	-225.3	267.4	41	27	-44	40	12.09	0.38	94	Y571	-525.8	177.1	173	27	228	28	13.22	0.31	6
FA80	21.0	136.3	30	17	-5	13	12.11	0.35	96	Y 88	279.5	133.7	71	19	117	25	13.22	0.21	84
Y247	486.7	-658.5	-30	20	45	21	12.12	0.06	95	Y 66	129.4	122.8	136	30	-86	38	13.23	0.47	71
Y549	-292.8	143.6	-18	24	-31	18	12.12	0.35	96	Y608	-270.7	334.9	-74	28	-30	27	13.24	0.62	93
FA26	-253.6	93.5	-42	17	-65	15	12.13	0.35	94	Y 44	126.4	233.6	10	17	44	26	13.24	0.27	96
Y397	-116.8	-402.1	-58	25	-12	32	12.14	0.62	95	Y467	-106.7	11.0	-105	22	36	28	13.25	0.37	90
Y447	-244.3	-163.3	91	19	37	19	12.15	0.21	92	Y269	184.6	-643.7	-6	15	-14	19	13.26	0.36	96
Y 4	-274.8	-443.0	-37	12	42	13	12.16	0.20	96	Y410	-223.5	-306.5	-179	22	150	22	13.26	0.28	25
Y158	407.4	-227.0	49	18	-48	18	12.17	0.22	95	Y556	-315.0	135.0	58	26	-72	26	13.27	0.44	92
FA18	-2.1	-378.9	27	19	-12	16	12.20	0.21	96	FB224	195.1	-368.3	-19	26	-34	28	13.27	0.49	96
Y327	-83.2	-631.4	88	14	-3	16	12.23	0.09	93	Y 40	219.4	250.1	-59	20	65	23	13.28	0.41	93
FA43	126.4	-253.5	483	24	-719	20	12.24	0.51	0	Y594	-405.9	248.4	325	26	-614	25	13.29	0.57	0
FA72	271.5	-326.3	-20	20	52	25	12.24	0.28	95	Y 50	-0.1	151.8	127	34	-31	25	13.29	0.36	83
FA55	379.3	-201.1	-18	19	-8	21	12.29	0.24	96	Y342	-103.7	-536.0	126	18	-766	21	13.29	0.53	0
Y491	-281.8	-44.4	0	17	114	23	12.29	0.36	90	Y487	-171.3	3.4	-14	40	-106	44	13.29	0.40	87
Y328	-102.6	-632.7	-1057	22	-265	17	12.30	1.03	0	FA40	207.4	-226.4	99	39	52	34	13.30	0.44	87
FA125	-196.8	62.3	97	23	-562	24	12.31	0.66	0	Y191	387.9	-365.2	55	20	89	25	13.30	0.36	91
Y548	-308.8	159.0	45	25	-58	30	12.34	0.29	94	FA53	311.7	-159.3	250	23	-163	31	13.32	1.23	3
FA33	305.3	-232.3	64	19	-117	19	12.36	0.26	86	Y 26	-7.7	232.6	16	47	69	29	13.32	0.28	93
Y 30	13.7	338.0	-59	18	-42	16	12.37	0.31	95	Y511	-286.1	82.6	-120	22	35	21	13.32	0.70	87
Y409	-247.4	-331.3	335	14	-688	15	12.40	0.64	0	Y315	-152.7	-752.4	160	19	-36	22	13.33	0.45	72
FA78	41.1	-113.7	-156	22	-27	28	12.40	1.11	74	Y 12	-76.5	304.2	22	31	91	23	13.33	0.35	92

TABLE 3. (continued)

Names	X	Y	μ_x	ϵ_x	μ_y	ϵ_y	V	B-V	P	Names	X	Y	μ_x	ϵ_x	μ_y	ϵ_y	V	B-V	P
	arcsec		milliarcsec cent^{-1}						%		arcsec		milliarcsec cent^{-1}						%
FA70	302.5	-312.1	20	22	-56	25	13.33	0.37	95	Y174	147.8	-352.6	250	27	-150	23	13.90	0.40	4
Y258	382.7	-524.3	-932	22	485	35	13.34	0.53	0	Y102	265.8	-73.5	-50	29	103	40	13.90	0.53	87
FA38	233.7	-228.9	-4	28	-178	37	13.35	0.39	64	Y470	-54.0	58.9	30	29	-40	28	13.92	0.34	95
Y120	202.0	-156.8	-57	27	-308	50	13.36	0.61	5	Y555	-298.4	127.3	-328	51	-143	40	13.92	0.69	1
Y601	-347.7	237.5	-81	35	-79	31	13.36	0.40	88	Y306	-35.5	-577.8	-117	32	-10	84	13.92	0.33	79
FB210	28.4	-134.3	330	22	-218	27	13.36	0.47	0	Y586	-291.3	434.5	316	73	846	77	13.93	0.43	0
Y559	-364.6	140.8	61	29	337	52	13.38	0.71	2	Y438	-124.9	-202.0	-171	48	-79	38	13.93	0.89	53
Y570	-433.0	152.1	4	29	34	23	13.39	0.25	96	Y465	-78.8	-18.1	97	31	94	40	13.93	0.52	81
Y193	415.0	-375.2	55	25	25	28	13.40	0.41	95	Y343	-80.2	-512.0	-44	30	-94	29	13.95	0.42	91
Y232	255.5	-520.5	-78	18	-75	22	13.40	0.24	91	Y577	-447.6	364.4	-887	41	217	32	13.95	0.58	0
Y 6	-111.0	417.4	-22	20	-15	27	13.40	0.27	96	Y363	94.6	-435.7	197	29	-25	32	13.96	1.20	47
Y 20	-7.8	115.9	-249	26	-52	28	13.42	0.51	13	Y325	-87.3	-671.3	-393	26	96	35	13.97	0.50	0
Y210	261.4	-425.3	-355	38	609	26	13.42	0.63	0	Y190	384.2	-352.2	26	30	-38	37	13.97	0.45	95
Y279	115.7	-778.1	-128	27	70	23	13.44	1.25	80	Y535	-203.6	195.0	-59	39	157	43	13.99	0.41	67
Y153	470.9	-316.7	28	21	4	20	13.46	0.33	96	Y308	33.2	-592.1	259	17	-25	28	14.00	0.39	9
Y536	-191.3	206.9	-1	27	15	28	13.46	0.40	96	Y207	308.1	-435.8	-26	26	11	26	14.01	0.35	96
Y215	191.2	-474.3	-63	24	-64	18	13.47	0.22	93	Y164	375.9	-326.5	120	22	-87	25	14.01	0.35	80
Y454	-357.5	-115.5	525	40	-132	27	13.47	0.50	0	FB211	3.8	-87.2	-505	35	-507	44	14.01	0.72	0
Y200	332.6	-402.0	55	24	71	29	13.47	0.45	93	Y352	118.0	-468.1	-27	24	-9	19	14.01	0.37	96
Y263	312.8	-536.6	-42	32	-67	29	13.47	0.52	93	Y337	-214.8	-529.3	385	28	-486	31	14.03	1.16	0
Y448	-321.7	-189.2	-358	23	-202	33	13.47	0.52	0	Y566	-343.0	108.1	-19	29	165	36	14.04	0.93	70
Y442	-201.3	-211.6	79	31	-144	33	13.49	1.22	71	Y 18	-81.9	188.9	16	28	73	32	14.05	0.33	94
FB207	9.1	-188.9	-104	52	84	43	13.50	0.68	78	Y456	-319.1	-112.4	517	24	-549	38	14.06	0.56	0
Y595	-406.5	175.6	-38	40	-182	38	13.50	0.48	58	Y290	150.4	-645.0	136	22	930	27	14.06	0.60	0
FB200	221.8	-299.5	14	26	-36	32	13.50	0.32	96	Y345	-44.0	-479.0	184	30	-37	26	14.07	0.38	56
Y 11	-68.8	328.3	34	27	26	26	13.51	0.32	96	Y277	126.3	-826.9	-69	20	-206	26	14.07	0.35	40
Y450	-307.9	-274.8	950	26	501	27	13.52	0.51	0	Y 19	-56.0	124.8	-30	28	69	43	14.07	0.63	93
FB248	-4.1	-466.4	-5	27	-18	27	13.52	0.30	96	Y525	-156.3	174.7	100	33	13	26	14.09	0.35	90
Y605	-320.0	287.6	-23	32	-5	33	13.52	0.32	96	Y553	-260.9	160.1	125	32	-101	70	14.10	0.51	66
Y394	-72.2	-412.7	-26	24	-30	29	13.52	0.31	96	Y557	-324.0	137.7	-17	37	-9	64	14.10	0.94	94
FA44	134.6	-184.2	-249	70	-13	36	13.52	0.63	25	Y552	-241.1	170.4	130	61	-226	66	14.11	0.87	20
Y149	522.3	-351.6	63	27	-20	43	13.52	0.59	94	Y 15	-73.0	227.8	-70	45	119	46	14.11	0.36	78
Y541	-219.6	262.3	101	76	-134	57	13.52	0.31	58	Y 34	60.7	383.0	10	27	81	28	14.12	0.37	93
Y357	105.8	-413.2	20	26	93	22	13.53	0.31	92	Y147	572.2	-318.3	56	32	32	26	14.12	0.45	94
Y508	-348.1	28.7	107	27	-60	34	13.53	0.53	86	Y213	221.2	-437.3	-125	30	59	25	14.13	0.29	82
Y324	-66.4	-697.8	-271	16	188	22	13.53	0.31	0	Y254	358.9	-612.8	509	22	-94	30	14.13	0.54	0
FB205	43.2	-288.9	-967	34	1044	35	13.55	0.87	0	Y206	334.8	-435.7	-34	26	6	30	14.13	0.45	96
FA56	-34.2	-276.7	-84	37	68	27	13.56	0.24	89	Y 47	23.4	192.3	-37	40	68	33	14.14	0.39	93
FB238	354.9	-325.0	64	24	-19	24	13.57	0.44	94	FB220	189.6	-224.4	70	37	-218	55	14.15	0.58	34
Y 17	-106.7	201.8	-3	24	79	28	13.57	0.29	94	Y180	207.8	-366.2	0	24	53	29	14.15	0.64	95
FA79	32.5	-125.0	44	25	-98	31	13.57	0.53	90	Y469	-64.5	39.6	-404	40	-31	41	14.16	0.78	0
Y418	-84.9	-242.4	-613	31	14	30	13.58	0.61	0	Y451	-443.6	-216.2	-3	30	-29	43	14.16	0.64	95
FA131	-126.3	162.9	2	26	-25	20	13.59	0.36	96	Y490	-283.9	-32.5	-232	52	-170	45	14.18	1.04	9
Y498	-538.7	9.0	-648	29	1506	26	13.59	0.51	0	Y104	285.8	5.6	-213	30	91	24	14.19	0.51	27
FB239	363.1	-304.1	6	31	-33	23	13.60	0.39	96	Y296	18.0	-552.5	50	34	-30	23	14.20	0.73	95
Y226	186.8	-548.1	3	25	-38	28	13.60	0.36	96	FA75	270.0	-351.4	-25	26	-71	27	14.20	0.58	94
Y502	-400.8	82.5	-15	40	-14	37	13.60	0.51	95	Y326	-84.1	-661.2	-2196	35	4522	33	14.20	1.08	0
Y 60	158.8	89.3	-34	26	5	27	13.60	0.41	96	Y234	392.5	-471.0	-379	25	139	25	14.22	0.56	0
Y256	407.0	-509.7	-18	22	-53	30	13.60	0.51	95	Y493	-438.8	-106.0	474	27	-465	27	14.23	0.48	0
Y257	381.5	-504.2	-94	23	-65	26	13.61	0.40	89	Y369	59.6	-344.8	-394	28	318	36	14.23	0.52	0
Y276	166.4	-795.1	135	22	1	18	13.61	0.16	84	Y293	121.8	-618.5	100	34	19	33	14.23	0.32	90
Y441	-225.2	-174.5	-1029	31	1735	34	13.62	0.61	0	Y240	548.2	-419.3	314	33	26	48	14.23	1.13	2
Y432	-16.9	-133.8	44	44	303	61	13.62	0.42	8	Y214	191.8	-460.4	-14	31	319	38	14.25	0.53	3
Y228	208.6	-594.7	39	22	-58	24	13.62	0.42	95	FB217	235.0	-140.6	-9	41	-18	37	14.25	0.70	96
Y 82	316.3	198.0	-811	34	-175	41	13.62	0.68	0	Y311	-34.4	-666.7	146	25	154	28	14.28	0.87	41
Y237	509.0	-474.8	67	28	-145	36	13.63	1.03	73	Y468	-49.7	20.9	-59	28	-52	37	14.29	0.52	93
Y 80	268.1	176.5	-12	28	-5	31	13.64	0.45	96	Y152	447.6	-339.2	-9	23	-37	19	14.29	0.40	96
Y 90	216.1	122.7	9	22	-44	25	13.64	0.39	96	Y527	-162.7	150.9	-342	616	708	415	14.29	0.77	2
Y598	-372.8	195.2	11	30	-26	34	13.66	0.62	96	Y437	-141.2	-182.8	17	29	4	37	14.30	0.67	96
Y505	-342.4	55.3	75	24	-12	32	13.67	0.43	94	Y230	240.4	-539.8	-885	40	371	59	14.31	0.70	0
Y270	184.3	-694.1	213	17	-208	27	13.67	1.15	3	Y299	-21.6	-562.7	-23	37	106	35	14.31	0.34	89
Y604	-342.3	264.0	-36	27	-16	39	13.68	0.34	95	Y415	-119.3	-260.0	1432	29	-430	35	14.31	0.71	0
Y593	-408.5	265.6	-818	49	748	31	13.68	1.23	0	Y255	396.7	-590.5	568	30	-223	41	14.31	0.55	0
Y253	406.5	-628.0	96	25	-37	27	13.69	0.47	91	Y333	-265.2	-596.5	20	30	-83	41	14.31	0.51	92
Y108	439.0	-97.9	468	31	60	29	13.70	1.41	0	Y 39	264.8	255.1	-164	29	-512	43	14.32	0.70	0
Y449	-314.3	-261.7	950	27	376	32	13.70	0.51	0	Y599	-362.5	194.9	-155	43	-74	49	14.33	0.55	61
Y411	-191.2	-332.9	287	33	32	32	13.70	0.50	5	Y 73	155.3	170.1	12	55	-33	50	14.33	0.31	94
FB216	210.1	-130.6	-1358	52	-39	71	13.71	1.02	0	Y 54	35.4	105.9	140	31	-14	43	14.33	0.37	79
Y512	-306.1	87.2	140	58	55	30	13.71	0.71	71	Y334	-300.7	-521.1	-745	36	-202	39	14.34	0.77	0
Y289	126.9	-653.7	20	23	99	25	13.71	0.29	92	Y127	186.1	-242.7	-62	41	30	39	14.34	0.56	93
Y359	95.9	-391.6	4	35	-46	28	13.71	0.33	95	Y109	379.5	-103.9	135	34	136	38	14.35	0.41	53
Y 41	193.7	262.7	-143	19	176	27	13.71	0.43	31	Y408	-281.9	-336.5	-285	32	-28	39	14.35	0.47	5
FB208	-0.7	-198.6	-64	29	-38	31	13.72	0.40	94	Y503	-369.4	48.7	-213	56	-14	35	14.36	0.67	39
Y455	-328.7	-118.3	580	24	-536	23	13.72	0.54	0	Y444	-231.4	-248.0	-37	46	-41	30	14.36	0.43	94
Y486	-175.4	8.2	-438	107	309	79	13.73	0.49	0	Y314	-85.4	-761.5	-99	45	240	29	14.37	0.95	15
Y264	296.5	-555.2	364	25	-191	32	13.74	0.43	0	Y294	88.1	-549.2	-124	26	140	29	14.37	0.56	58
Y416	-144.9	-249.1	32	31	176	30	13.75	0.42	64	Y249	467.2	-590.0	-194	18	-349	28	14.37	0.54	0
Y 29	-3.9	321.2	-47	21	185	23	13.75	0.28	59	Y 8	-76.2	390.4	-822	34	90	52	14.39	0.50	0
Y350	67.5	-478.3	115	32	38	27	13.75	0.34	86	Y414	-141.8	-279.2	118	47	-101	36	14.39	0.67	71
Y150	521.1	-359.5	-5	26	-59	37	13.77	0.53	95	Y616	-256.7	307.9	2	43	17	52	14.40	1.02	95
Y531	-230.4	161.2	-52	94	141	57	13.77	0.40	62	Y 93	145.6	-57.7	66	44	-166	33	14.40	0.57	62
Y196	403.6	-403.3	74	26	-114	27	13.77	0.44	84	Y 14	-79.3	235.2	-77	39	20	41	14.41	0.65	92
FB206	22.3	-300.4	26	25	43	28	13.78	0.45	95	Y501	-424.5	95.0	-2	30	-133	39	14.42	0.44	83
Y592	-421.4	279.3	-190	26	-16	37	13.80	0.63	53	Y 97	74.3	-128.6	81	33	27	33	14.42	0.35	92
FB240	368.3	-293.3	24	27	59	20	13.82	0.41	95	Y521	-186.4	117.0	-44	48	24	42	14.42	0.39	94
FA62	37.0	-413.9	113	25	22	25	13.84	0.29	89	Y338	-175.5	-503.5	-109	38	91	36	14.42	0.90	78
Y188	317.0	-377.7	-9	20	-56	32	13.84	0.55	95	Y134	410.4	-177.7	-31	33	35	39	14.43	0.48	95
Y539	-156.3	282.7	18	41	39	42	13.84	0.81	95	Y197	396.9	-412.7	150	30	-58	35	14.44	0.70	71
Y283	-10.4	-736.2	-1049	22	271	20	13.85	0.63	0	Y607	-309.1	307.4	29	57	-157	39	14.45	0.59	69
Y241	572.2	-420.5	-39	27	10	24	13.85	0.30	96	Y157	419.4	-278.1	-217	35	17	28	14.45	0.28	35
Y 69	74.8	164.0	6	27	17	30	13.85	0.33	96	Y585	-293.3	430.1	-384	325	-2423	602	14.46	0.51	0
Y609	-250.0	352.5	-827	39	649	51	13.85	0.92	0	Y 10	-67.7	358.2	223	39	-231	48	14.46	1.24	3
Y205	344.6	-438.0	-193	57	224	32	13.86	0.66	6	Y340	-132.1	-492.0	-114	38	-204	37	14.46	0.65	29
Y 91	214.4	56.7	-200	39	54	37	13.88	0.60	42	Y459	-270.1	-106.8	-111	31	-169	45	14.46	0.38	48
Y492	-393.5	-44.9	-74	28	50	26	13.88	0.25	92	Y591	-409.6	294.3	-69	33	149	45	14.47	0.84	69
Y517	-219.1	130.2	195	33	15	34	13.88	0.50	49	Y612	-158.0	395.3	-122	58	295	57	14.48	0.40	5
FB204	96.8	-323.9	119	41	-2	26	13.89	0.36	85	Y316	-129.7	-744.9	344	27	-46	22	14.48	0.45	0
Y615	-224.1	330.4	-165	36	53	33	13.89	0.41	63	Y614	-183.4	331.4	-791	54	-169	49	14.49	0.77	0
Y529	-210.8	149.6	54	45	-56	37	13.90	0.37	92	Y457	-320.8	-127.3	-497	30	-233	35	14.50	0.89	0
Y358	94.1	-398.6	56	32	-66	44	13.90	0.35	91	Y177	166.2	-404.9	2075	40	-1072	43	14.51	0.70	0

TABLE 3. (continued)

Names	X	Y	μ_x	ϵ_x	μ_y	ϵ_y	V	B-V	P	Names	X	Y	μ_x	ϵ_x	μ_y	ϵ_y	V	B-V	P
	arcsec		milliarcsec cent^{-1}						%		arcsec		milliarcsec cent^{-1}						%
Y 78	227.8	201.0	-22	31	23	26	14.51	0.39	96	Y148	544.5	-346.0	-90	31	6	35	14.91	0.34	92
Y159	390.1	-236.7	222	46	57	42	14.52	0.83	29	Y313	-67.2	-724.3	709	31	-80	26	14.91	0.40	0
Y603	-380.3	267.6	-219	41	74	70	14.52	0.52	25	Y242	573.2	-433.1	541	27	-786	45	14.91	0.53	0
Y462	-136.5	-88.0	-38	40	102	44	14.52	0.38	87	Y 24	-12.8	180.7	-19	32	70	50	14.92	0.39	92
Y181	212.9	-383.0	-617	40	-148	26	14.52	0.57	0	Y440	-186.0	-154.1	-562	74	464	68	14.93	0.74	0
Y135	569.1	-189.6	25	31	-35	28	14.52	0.55	95	Y252	402.4	-618.9	-367	20	-17	30	14.94	0.50	0
Y 96	98.8	-131.3	113	59	-115	46	14.53	0.49	65	Y405	-401.2	-336.7	-70	22	45	28	14.94	0.50	93
Y590	-337.[illegible]	331.0	-99	36	-51	38	14.53	0.35	87	Y435	-89.7	-130.5	-44	32	-102	41	14.94	0.44	88
Y423	49.4	-152.7	104	66	140	63	14.53	0.37	56	Y167	329.1	-275.6	739	66	-13	58	14.94	0.70	0
Y103	251.4	12.7	-589	33	32	39	14.54	0.48	0	Y319	-182.4	-699.4	-1	44	45	35	14.95	0.34	95
Y295	47.3	-563.2	48	25	-144	22	14.54	0.31	80	Y156	455.8	-221.5	-994	52	429	52	14.95	0.63	0
Y506	-315.6	46.2	21	58	-66	46	14.54	0.42	91	Y332	-177.5	-604.0	35	29	-239	30	14.96	0.46	24
Y600	-360.0	232.8	-688	50	228	89	14.54	1.00	0	Y143	544.9	-203.7	-35	37	-90	50	14.96	0.59	89
Y578	-452.9	390.0	-15	43	-151	70	14.54	0.36	68	Y580	-407.8	379.5	-232	60	-362	83	14.96	0.60	0
Y318	-225.8	-688.0	303	56	230	69	14.56	0.62	1	Y504	-351.5	49.5	-57	72	8	58	14.96	0.49	88
Y 55	57.5	103.4	152	45	-205	54	14.56	0.71	20	Y341	-147.0	-513.3	104	22	-12	41	14.97	0.57	90
Y271	277.7	-710.3	142	32	28	23	14.58	0.37	79	Y355	138.4	-430.2	-29	75	151	70	14.98	0.69	63
Y105	403.6	-0.1	140	22	-177	34	14.58	1.08	32	Y 25	-35.1	242.4	105	39	127	59	14.98	0.57	65
Y606	-320.9	306.3	62	38	32	40	14.58	0.43	93	Y265	305.9	-568.8	-10	31	-11	40	14.99	0.54	96
Y243	579.8	-572.9	-533	101	1092	98	14.58	0.52	0	Y250	445.2	-615.3	-356	32	89	28	14.99	0.62	0
Y404	-342.5	-350.9	345	32	-80	39	14.59	0.71	0	Y446	-251.6	-198.1	150	43	-505	45	14.99	0.47	0
Y574	-515.2	309.1	-29	80	222	59	14.59	0.52	32	Y101	231.3	-34.4	-968	36	640	63	14.99	0.56	0
Y111	383.6	-134.4	37	41	-1052	30	14.59	0.59	0	Y407	-358.6	-307.9	74	27	89	30	15.00	0.41	88
Y596	-400.5	178.3	-18	90	-41	37	14.60	0.60	89	Y354	137.6	-439.5	-262	86	-144	54	15.00	0.53	12
Y568	-415.7	116.7	44	42	32	47	14.60	0.60	94	Y 83	330.6	188.1	-136	52	33	44	15.00	0.37	74
Y244	547.6	-601.5	-129	45	132	42	14.61	0.44	56	Y300	-35.4	-569.0	-33	60	-58	35	15.00	0.48	92
Y291	169.1	-614.7	-159	29	53	37	14.61	0.46	67	Y220	162.9	-560.8	12	48	26	44	15.01	0.35	95
Y235	433.5	-451.3	40	42	26	25	14.61	0.41	95	Y 57	21.7	37.0	-360	62	820	133	15.01	0.52	0
Y386	-54.3	-334.9	122	26	19	30	14.61	0.52	86	Y569	-489.2	108.5	110	45	-83	58	15.01	0.39	75
Y248	462.8	-611.7	-107	21	127	33	14.62	0.45	71	Y 86	312.9	88.9	-33	48	-42	32	15.01	0.38	94
Y268	263.0	-613.3	28	32	-40	30	14.62	0.39	95	Y218	168.1	-533.4	264	30	-27	38	15.03	0.43	10
Y335	-296.6	-490.9	-7	25	-229	28	14.63	0.46	32	Y 37	259.8	334.5	-169	44	32	47	15.03	0.64	61
Y 74	162.5	140.0	92	44	-32	40	14.63	0.60	89	Y589	-321.8	360.6	129	40	-25	74	15.03	0.51	75
Y146	615.7	-342.2	1670	35	-792	34	14.63	0.60	0	Y479	-167.6	61.2	82	86	-21	74	15.04	0.46	79
Y186	284.1	-360.8	-396	125	-996	119	14.63	0.40	0	Y588	-310.4	369.1	-223	64	88	47	15.04	0.55	27
Y 52	33.9	140.7	117	82	128	66	14.65	0.90	54	Y 59	143.7	48.0	-390	68	-1737	75	15.05	0.72	0
FB236	171.7	-196.2	-305	69	427	74	14.65	0.85	0	Y430	17.3	-105.0	13	86	-676	39	15.05	0.52	0
Y219	170.5	-540.3	363	36	-163	33	14.66	0.66	0	Y466	-102.0	-18.5	-59	72	193	85	15.06	0.45	44
Y282	-18.0	-794.4	-62	32	-162	32	14.66	0.57	67	Y 13	-109.5	319.0	-828	48	326	51	15.06	0.51	0
Y507	-327.6	29.4	-105	40	318	67	14.67	0.58	5	Y540	-186.4	284.4	-199	63	92	86	15.06	0.36	33
Y400	-147.3	-443.5	30	35	-158	33	14.68	0.44	73	Y 43	107.3	264.0	334	37	-149	60	15.06	0.68	0
Y419	-92.1	-215.8	-158	34	84	44	14.68	0.52	59	Y298	-16.2	-531.7	-77	52	-130	65	15.08	0.41	68
Y458	-277.5	-130.6	11	40	44	47	14.68	0.29	94	Y 81	321.8	237.9	25	45	-16	48	15.08	0.50	95
Y522	-182.9	140.2	296	50	-54	43	14.69	0.41	6	Y510	-259.4	27.1	151	66	-10	109	15.09	0.51	55
Y573	-496.8	245.9	-497	57	125	72	14.69	0.48	0	Y117	239.8	-191.4	-42	76	138	58	15.09	0.51	68
Y495	-458.3	-31.8	589	33	-154	28	14.69	0.44	0	Y195	445.9	-374.2	74	42	-1	27	15.09	0.44	93
Y145	581.2	-241.0	-7	35	-299	25	14.70	0.40	3	Y368	21.9	-379.3	289	49	-51	47	15.10	0.56	7
Y538	-152.0	242.3	-18	34	50	44	14.70	0.47	94	Y583	-332.9	384.3	39	83	21	75	15.10	0.72	86
FB225	169.8	-339.8	177	89	292	72	14.70	0.58	5	Y477	-26.7	65.1	7	63	-20	50	15.11	0.51	93
Y275	138.0	-746.8	88	28	-270	29	14.70	0.39	7	Y464	-126.5	-37.8	135	68	-80	44	15.11	0.49	65
Y584	-309.4	403.5	-39	64	82	65	14.72	0.48	84	Y339	-176.1	-493.1	-98	42	-99	41	15.12	0.53	78
Y587	-288.8	380.2	-314	51	230	52	14.72	0.61	0	Y262	338.6	-552.0	-270	34	386	34	15.12	0.54	0
Y 94	98.6	-84.5	734	35	437	79	14.72	0.70	0	Y329	-117.3	-619.4	-27	53	63	39	15.12	0.32	92
Y439	-160.2	-142.6	191	60	192	52	14.72	0.66	15	Y 84	350.8	146.1	-239	77	-507	46	15.12	0.44	0
Y460	-206.9	-97.5	-52	39	-50	39	14.73	0.88	93	Y330	-133.7	-649.3	73	41	-68	48	15.12	0.48	88
Y141	588.0	-195.9	-391	23	211	35	14.73	0.46	0	Y402	-229.9	-409.2	193	32	12	52	15.13	0.53	48
Y 7	-102.8	398.3	-117	47	6	26	14.73	0.35	84	Y572	-524.0	216.1	-101	58	82	47	15.13	0.46	77
Y312	-29.2	-694.8	-296	22	10	27	14.75	0.56	2	Y431	-19.3	-118.5	169	99	-137	68	15.13	0.37	36
Y526	-161.1	158.0	74	41	4	75	14.75	0.48	89	Y 32	4.4	387.1	-226	60	-50	64	15.13	0.47	28
Y 31	-0.5	397.2	-76	33	202	38	14.76	0.40	40	Y 58	93.4	50.4	24	45	-32	62	15.13	0.55	93
Y229	211.3	-607.0	-258	32	64	49	14.79	0.48	10	Y434	-81.8	-170.2	366	57	-229	86	15.13	0.61	0
Y385	-26.0	-351.6	196	49	187	54	14.79	0.54	14	Y370	83.5	-355.4	436	50	-65	51	15.14	0.54	0
Y 35	208.7	361.8	-45	43	-6	41	14.80	0.51	94	Y497	-502.7	-62.2	-1106	49	-235	42	15.15	0.50	0
Y484	-214.8	39.4	-236	67	-44	61	14.81	0.57	26	Y429	-4.0	-54.3	-240	57	333	93	15.15	0.55	1
Y246	496.3	-643.8	-26	34	157	36	14.81	0.32	73	Y347	-9.4	-481.3	342	89	-198	71	15.15	0.55	2
Y387	-55.8	-308.4	-4	45	22	40	14.83	0.45	95	Y236	445.6	-445.3	-523	39	241	39	15.17	0.42	0
Y575	-478.8	346.1	137	58	35	47	14.83	0.37	72	Y310	-20.9	-640.3	259	36	99	40	15.18	0.37	8
Y515	-255.9	120.8	424	94	-15	77	14.84	0.62	1	Y239	527.0	-433.3	-2	41	-22	41	15.18	0.29	95
Y281	25.0	-797.0	135	37	77	25	14.84	0.64	74	Y417	-122.0	-245.2	-681	53	262	45	15.19	0.52	0
Y567	-392.8	111.2	239	61	-128	64	14.84	0.52	15	Y 77	224.3	195.1	405	29	-76	64	15.20	0.66	0
Y 36	220.4	335.9	67	48	-331	58	14.86	0.68	3	Y496	-506.4	-28.0	-182	48	-12	34	15.21	0.40	56
Y403	-291.2	-360.9	48	39	-221	48	14.86	0.50	35	Y478	-79.8	98.3	250	56	6	52	15.22	0.48	21
Y160	373.2	-252.3	328	57	-116	37	14.86	0.61	2	Y554	-291.6	119.6	-661	76	-173	77	15.23	0.63	0
Y336	-272.6	-489.9	-333	29	177	23	14.87	0.38	0	Y144	565.8	-244.8	-45	49	41	37	15.24	0.46	93
Y367	5.6	-369.0	241	62	-28	40	14.87	0.47	26	Y463	-115.1	-104.1	-838	51	825	79	15.25	0.55	0
Y251	415.5	-612.7	-203	21	232	28	14.87	0.55	2	Y 22	-53.4	178.6	-413	99	-77	63	15.26	0.46	2
Y485	-202.3	40.5	-74	58	-81	71	14.87	0.61	79	Y576	-459.6	359.8	4	78	22	77	15.27	0.46	88
Y112	324.9	-133.8	-108	42	17	42	14.88	0.59	86	Y217	174.7	-530.0	-34	51	41	57	15.28	0.35	92
Y401	-242.6	-436.8	5	29	-18	29	14.88	0.59	96	Y 42	113.0	266.6	-12	72	114	74	15.28	0.48	75
Y274	168.3	-730.3	-188	51	-289	54	14.88	0.47	2	Y 79	252.7	185.1	-121	43	65	43	15.28	0.34	78
Y488	-227.4	-4.5	352	53	-21	53	14.88	0.57	1	Y412	-134.2	-315.5	-386	113	280	100	15.29	0.51	1
Y194	426.0	-375.6	-83	39	-28	31	14.89	0.39	91	Y 72	143.1	175.0	-87	52	90	73	15.31	0.38	76
Y278	116.6	-789.7	-606	34	831	36	14.89	0.75	0	Y 46	66.8	225.1	-190	96	34	121	15.32	0.42	38
Y518	-218.6	117.1	49	74	146	80	14.90	0.91	61	Y 85	359.1	87.5	114	49	31	46	15.35	0.34	82
Y231	250.9	-565.2	-7	37	-73	42	14.90	0.42	93	Y406	-367.0	-333.2	-420	40	462	40	15.36	0.35	0
Y597	-401.2	151.4	-254	42	366	53	14.90	0.56	0	Y175	155.6	-383.0	-60	72	237	48	15.40	0.29	23
Y393	-90.6	-375.9	21	84	-252	68	14.90	0.49	22	Y176	162.4	-392.5	249	59	227	74	15.49	0.33	4
Y309	33.9	-637.0	-376	55	76	44	14.90	0.49	0										
Y323	-88.8	-708.2	-52	31	116	20	14.90	0.37	87										
Y 89	246.8	130.5	113	34	-111	43	14.91	0.56	71										

atic errors in our photometry. In contrast, it is extremely difficult to derive reliable reddenings and hence distance moduli for the clusters from our data alone, without using spectral types or color–color plots. Comparing with the zero-age main sequence (ZAMS) of Mihalas & Binney (1981), we find our CMD's are consistent with $E(B-V)\sim 0.5$ (but highly variable) and $(m-M)_0 \approx 12.5$ as derived from spectra and better photometric data by Massey & Johnson (1993), but are also consistent with a variety of other reddenings and distances. This compari-

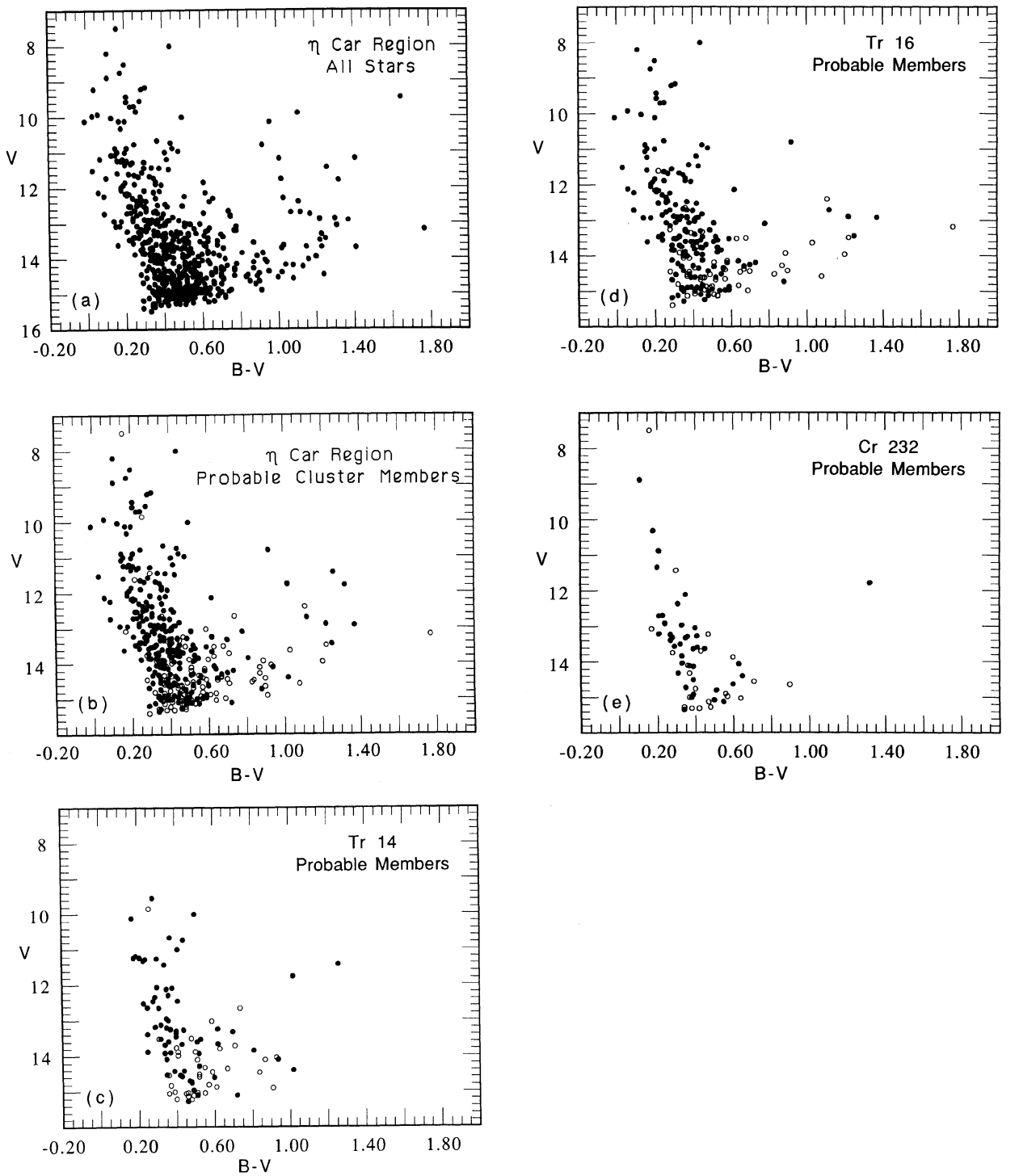

FIG. 2. Color–magnitude diagram of all stars measured in the region of η Car, regardless of membership probability. (b) Color–magnitude diagram of probable cluster members. Stars with astrometric membership probability $P \geqslant 80\%$ are indicated by filled circles while those with $20\% \leqslant P < 80\%$ are shown as open circles. (c) As in (b) but for stars in the region of Tr 14 only. (d) As in (b) but for stars in the region of Tr 16 only. (e) As in (b) but for stars in the region of Cr 232 only.

son, of course, is sensitive to any possible systematic errors in our photometry.

Some comments are in order for several stars in each of the CMD's. The Wolf–Rayet star HD 93162 lies in the region of Tr 16 and has $P=93\%$. Tr 16 also contains several probable members which have quite red $B-V$ colors. Inspection of the original plates reveals them to be unremarkable images, although stars Y397, Y398, and Y399

are located close to each other and in what appears to be a fairly dense dust lane. One of these stars, Y398 at $V \approx 10.80$ with $P = 89\%$, was recently discovered by Massey & Johnson (1993) to have the unexpected spectral type of O3–O4If (their star 257). In Tr 14, stars Y581 and Y582 (in the northwest corner of Tr 14) are spatially close and also in an apparently dusty area. Cr 232 contains one star, Y56, with an unusually large color index, also in an apparently dusty region. Feinstein (1982) also found stars lying to the right in his dereddened CMD. Of the nine candidates in group (a) of his Table VI, we identified five in common with our observations (Nos. 200, 204, 206, 208, and 210). Four of the five candidates have high membership probability ($P > 80\%$) and one has zero membership probability. Hence for these stars we conclude that Feinstein's suggestion that they are pre-ZAMS stars still in the process of gravitational contraction to be plausible and that they are probably not merely nonmembers contaminating the CMD.

Our criterion for distinguishing members from nonmembers is based exclusively on proper motions. It is useful to inquire as to how other criteria compare with ours. Feinstein *et al.* (1973) analyzed the color–color diagram to separate the cluster stars from the field stars. Their technique will tend to classify as field stars those for which reddening is unusually small (in this differentially reddened region) and also stars whose photometry is in error due to nebular contamination. Of 132 stars in his sample, we identified 87 for which we have proper motions. Of these Feinstein considered 78 to be members. We found 65 to be proper motion members ($P > 80\%$) and 6 to be likely nonmembers ($P < 20\%$). Hence his member star sample agrees well with ours. However, some stars he considered to lie in the foreground appear to be proper motion members. We found 9 of his foreground stars to be in common with our sample, and of those, 6 (FA20, 48, 56, 58, 69, and 94) have high membership probabilities ($P > 90\%$) and 3 (FA32, 125, HD 93268) have zero membership probability. Photometric errors due to nebular contamination appear to be possible for some of the stars for which we disagree, but we also remind the reader that on statistical grounds we expect some field stars to have high membership probabilities.

In another survey, Smith (1987) used near-infrared photometry to separate out the member stars. His sample was somewhat smaller than Feinstein's but we were able to identify 12 of his member stars. We found 8 to have $P > 80\%$ and 2 to have $P < 20\%$. Thus these previous authors appear to have been fairly successful in separating members from nonmembers when compared to our proper motion study, although some discrepancies exist which should not affect those previous studies significantly.

There are a few bright blue stars in Table 3 for which we derived moderately large relative proper motions and hence low or zero membership probabilities (HD 93268, Y494, FA32, and Y2). Two of these were noted above as having been classified as field stars by Feinstein *et al.* (1973) based on their color–color plot. Simple inspection of a $(V, B-V)$ CMD would imply that these stars could well be cluster members. Massey & Johnson (1993) have obtained $U-B$ colors for all 4 of these stars as well as $B-V$, however, and their locations in the color–color plot are most consistent with their being lightly reddened foreground stars (at distances ~ 1 kpc) with spectral types near A0, in accord with our astrometric results. As further evidence of this, HD 93268 was classified as A2 many decades ago in the HD catalog.

Inspection of Table 3 or application of the parameters of Table 2 shows that a star requires a proper motion $> 0\farcs2$ cent^{-1} relative to the cluster to have a low or zero membership probability. At the clusters' distance ~ 3 kpc this corresponds to a tangential velocity > 30 km s^{-1} relative to the clusters. Thus most nonmember young stars at such distances will probably not be distinguishable from cluster members via our proper motions. Field stars that are older (and hence have generally larger velocities) or nearer are more easily distinguished from the cluster, as demonstrated by Figs. 2(a) and 2(b) and by the foreground A stars discussed above. Some of the scatter in the cluster CMD's and some discrepancies between photometric and astrometric membership could thus be due to young field stars at distances roughly similar to the clusters rather than to differential reddening or photometric uncertainties. Turner & Moffat (1980) found evidence for young stars as near as 2.1 kpc and as distant as 4.9 kpc in an extended annulus around Cr 228, about 30′ south of our field. If there are such stars in our field their proper motions might not show them to be nonmembers.

4.2 Variable Stars

Motivated by the identification by Feinstein *et al.* (1973) of some variable stars within Tr 14 and Tr 16, a search for variable star candidates in this survey was carried out. We plotted the accidental errors (derived from the plate-to-plate scatter) in our B and V against the respective magnitude and looked for stars with unusually large errors compared to others at similar magnitude. We found no stars to stand out significantly. Identification on these plots of the previously known variable stars revealed them to have errors of $\epsilon_V \lesssim 0.01$ and $\epsilon_B \lesssim 0.07$, which would be quite unusual if the stars really vary by as much as ~ 0.5 mag. Given that the plates were taken over a time scale of about a day at each of the epochs, we conclude that there exists no evidence for variability of these stars on such a time scale. We cannot, of course, rule out variability on other time scales. Since Feinstein *et al.* gave very little discussion of these stars beyond noting V variations from 0.14 to 1.34 mag, over unspecified time scales, we cannot say whether or not our failure to find variability is a true discrepancy with their work.

4.3 Kinematic Association of the Clusters

As noted above, there has been some controversy historically as to whether these clusters all lie at a common distance and are mutually associated. We have argued above that the CMD's imply they all lie at a common distance. To investigate their kinematic association we

have derived the mean relative proper motions of the probable members ($P > 90\%$) in each of the three clusters. The means are not significantly different from zero, with errors of the mean ranging from about 3 to about 6 mas cent^{-1} (corresponding to velocities of 0.4 to 0.7 km s^{-1} at a distance $\sim$2.5 kpc). This appears to be strong evidence for common kinematics (to better than 1 km s^{-1}) among all 3 clusters, and hence for their association. We must caution, however, that this may not be as firm a conclusion as it appears. The plate constant reductions could have removed real differences in proper motions. As a simple example of this, note that an expansion of the clusters from a central point would have closely resembled a scale change of the plates, and would thus have been taken out by the plate constants.

It is useful to examine the spatial distribution of probable members. We find that both Tr 14 and Cr 232 have a fairly uniform distribution of member ($P > 80\%$) and nonmember ($P < 20\%$) stars (though Tr 14 has an obvious very strong clump in its center where stars were too crowded for us to measure). Tr 16 shows several distinct regions where almost all the stars have a high membership probability. In particular, the region extending 5′ south and 2′ north of η Car itself has a very high concentration of members (95% of the stars measured in this region have a membership probability $> 90\%$). There are also three less distinct such groupings approximately 4′ west of η Car. Owing to an obscuring dust lane, few stars lie between these major groups. Based on these observations, we conclude that the stars most clearly associated with Tr 16 can be enclosed by a circle of radius $\sim$4′ centered on η Car itself.

5. CONCLUSIONS

Photometry and astrometry have been presented for 577 stars in the Carina complex near η Car, including the clusters Tr 14, Tr 16, and Cr 232. Similarities in the CMD's of the clusters, along with the small proper motion differences, lend strong support to the notion that these three clusters are physically associated. Analysis of the CMD's of Tr 14 and Tr 16 in particular reveals no shift between these clusters. We thus find no evidence for the suggestion that Tr 14 is actually further away than Tr 16. A search for variable stars among all the stars in this survey revealed no clear candidates with variability on time scales $\sim$1 day.

Special thanks to Nick Suntzeff and Steve Majewski for obtaining the Las Campanas plates used in this study and to Martha Hazen for the loan of the Harvard plates. S.C.M. also wishes to express thanks to John Smetanka for many stimulating and invigorating discussions. As always, the hospitality of the University of Wisconsin during our use of the MADRAF facilities is much appreciated. This research has been partially supported by the NSF. Phil Massey kindly provided an early preprint of his recent work as we were completing our study.

REFERENCES

Cudworth, K. M. 1976, AJ, 81, 519
Cudworth, K. M. 1985, AJ, 90, 65
Cudworth, K. M. 1986, AJ, 92, 348
Cudworth, K. M., & Rees, R. 1991, PASP, 103, 470
Feinstein, A. 1982, AJ, 87, 1012
Feinstein, A., Marraco, H. G., & Muzzio, J. C. 1973, A&AS, 12, 331
Forte, J. C., & Orsatti, A. M. 1981, AJ, 86, 209
Garcia, B., Claria, J. J., & Levato, H. 1988, Ap&SS, 143, 317
Herbst, W. 1976, ApJ, 208, 923
Levato, H., & Malaroda, S. 1982, PASP, 94, 807
Massey, P., & Johnson, J. 1993, AJ, 105, 980
Mihalas, D., & Binney, J. 1981, Galactic Astronomy (Freeman, New York), p. 106
Morrell, N., Garcia, B., & Levato, H. 1988, PASP, 100, 1431
Smith, R. G. 1987, MNRAS, 227, 943
Tapia, M., Roth, M., Marraco, H., & Ruiz, M. T. 1988, MNRAS, 232, 661
Turner, D. G., Grieve, G. R., Herbst, W., & Harris, W. E. 1980, AJ, 85, 1193
Turner, D. G., & Moffatt, A. F. J. 1980, MNRAS, 192, 283
Vasilevskis, S., Klemola, A., & Preston, G. 1958, AJ, 63, 387
Walborn, N. R. 1973, ApJ, 179, 517
Walborn, N. R. 1982, AJ, 87, 1300

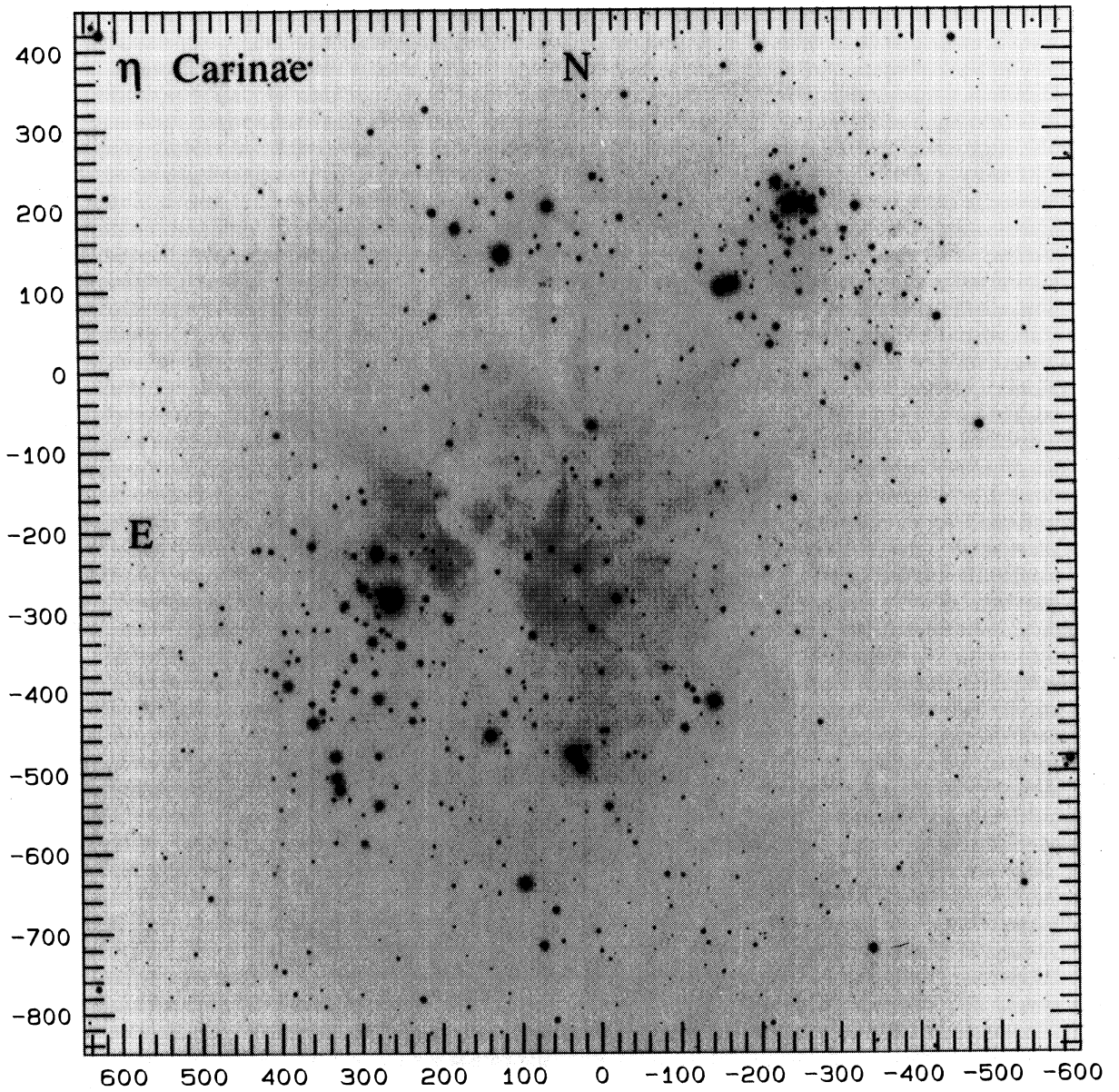

FIG. 1. Identification chart for stars measured in the region of η Car. North is at the top, and east to the left. The offset coordinates listed in Table 3. Tr 14 is centered near (−250, +200), Cr 232 near (+100, +180), and Tr 16 includes most of the field south of $y=0$. η Car is the very bright image at (+260, −285). A useful chart identifying the clusters can be found in Turner & Moffat (1980).

Cudworth *et al.* (see page 1823)